Topographic control of snowpack distribution in a small catchment in the central Spanish Pyrenees: intra- and inter-annual persistence

J.Revuelto[1], J.I. López-Moreno[1], C. Azorin-Molina[1], S.M. Vicente-Serrano[1]

[1] Instituto Pirenaico de Ecología, Consejo Superior de Investigaciones Científicas (IPE-CSIC) Departamento de Procesos Geoambientales y Cambio Global, Campus de Aula Dei, P.O. Box 13034, 50059, Zaragoza, Spain

Email addresses: jrevuelto@ipe.csic.es, nlopez@ipe.csic.es, cazorin@ipe.csic.es, svicen@ipe.csic.es

* Corresponding author: jrevuelto@ipe.csic.es

Abstract:

In this study we analyzed the relations between terrain characteristics and snow depth distribution in a small alpine catchment located in the central Spanish Pyrenees. Twelve field campaigns were conducted during 2012 and 2013, which were years characterized by very different climatic conditions. Snow depth was measured using a long range terrestrial laser scanner and analyses were performed at a spatial resolution of 5 m. Pearson's r correlation, multiple linear regressions (MLRs) and binary regression trees (BRTs) were used to analyze the influence of topography on the snow depth distribution. The analyses were used to identify the topographic variables that best explain the snow distribution in this catchment, and to assess whether their contributions were variable over intra- and inter-annual time scales. The topographic position index (index that compares the relative elevation of each cell in a digital elevation model to the mean elevation of a specified neighborhood around that cell with a specific shape and searching distance), which has rarely been used in these types of studies, most accurately explained the distribution of snow. The good capability of TPI to predict snow distribution has been observed in both, MLRs and BRTs, for all analyzed days. Other variables affecting the snow depth distribution included the maximum upwind slope, elevation, and northing. The models developed to predict snow distribution in the basin for each of the 12 survey days were similar in terms of the explanatory variables. However, the variance explained by the overall model and by each topographic variable, especially those making a lesser contribution, differed markedly between a year in which snow was abundant (2013) and a year when snow was scarce (2012), and also differed between surveys in which snow accumulation or melting conditions dominated in the preceding days. The total variance explained by the models clearly decreased for those days on which the snowpack was thinner and more patchily. Despite the differences in climatic conditions in the 2012 and 2013 snow seasons, similarities in snow distributions patterns were observed which are directly related with terrain topographic characteristics.

Keywords: snow depth distribution, snowpack evolution, topography, mountains, cold region

1. Introduction

Assessing the snow distribution in mountain areas is important because of the number of processes in which snow plays a major role, including erosion rates (Pomeroy and Gray, 1995), plant survival (Keller et al., 2000; Wipf et al., 2009), soil temperature and moisture (Groffman et al., 2001), and the hydrological response of mountain rivers (Bales and Harrington, 1995; Barnett et al., 2005; Liston, 1999; Pomeroy et al., 2004). As mountain areas are highly sensitivity to global change (Beniston, 2003), snow accumulation and melting processes are likely to be subject to marked changes in coming decades, affecting all processes influenced by the presence of snow (Caballero et al., 2007; López-Moreno et al., 2011, 2012b; Steger et al., 2012). For these reasons, much effort has been devoted to understanding the main factors that control the spatial and temporal dynamics of snow (Egli et al., 2012; López-Moreno et al., 2010; Mott et al., 2010; Schirmer et al., 2011).

One of the main difficulties in snow studies is obtaining reliable information of the variables that describe snow distribution, including snow depth (SD), snow water equivalent (SWE) and snow covered area (SCA). Manual measurements have traditionally been used to provide information on the distribution of snowpack, with different sampling strategies having been applied at various spatial scales (Jost et al., 2007; López-Moreno et al., 2012a; Watson et al., 2006). However, manual sampling is not feasible for large areas because of the time involved, especially when SWE measurements are also acquired. In the last decade the use of airborne laser scanners (ALS) (Deems et al., 2006) and terrestrial laser scanners (TLS) (Prokop, 2008), both of which are based on LiDAR (light detection and ranging) technology, have provided for major advances in obtaining data on the SD distribution at unprecedented spatial resolutions. These developments have enabled studies of several factors that in the past have been only marginally considered, including scaling issues (Fassnacht and Deems, 2006; Mott et al., 2011; Schirmer and Lehning, 2011; Trujillo et al., 2007), the detailed dynamics of snow

74   accumulation and ablation (Grünewald et al., 2010; Schirmer et al., 2011; Scipión et al.,

75   2013), and snow transport processes (Mott et al., 2010). In addition, the high density

76   measurements provided by LiDAR technologies are a valuable resource for detailed

77   investigation of the linkage between snow distribution and topography. In the past, this

78   linkage has mostly been studied using manual measurements, and hence with generally

79   limited spatial and temporal resolution (López-Moreno et al., 2010).

80   Previous studies have highlighted the marked control of topography on snow distribution in

81   mountain areas (Anderton et al., 2004; Erickson et al., 2005; Lehning et al., 2011; Mott et al.,

82   2013), and the importance of vegetation and wind exposure (Erxleben et al., 2002; Trujillo et

83   al., 2007). The most commonly used approach has been to develop digital elevation models

84   (DEM) that describe the spatial distribution of elevation, from which other terrain variables

85   are derived such as slope, terrain aspect, curvature, wind exposure or sheltering, and potential

86   solar radiation. This enables to analyze the linear or non-linear relation of these variables to

87   punctual SD or SWE values to be established (Grünewald et al., 2010; Schirmer et al., 2011).

88   Various statistical methods have been applied for this purpose, including linear regression

89   models (Fassnacht et al., 2003; Hosang and Dettwiler, 1991), generalized additive models

90   (GAM) (López-Moreno and Nogués-Bravo, 2005), and binary regression trees (BRT)

91   (Breiman, 1984) which have been widely applied in a diversity of regions (Elder et al., 1991;

92   Erxleben et al., 2002; McCreight et al., 2012).

93   The extent to which topographic variables explain snow distribution can change during the

94   snow season; the variability of terrain characteristics can drive processes related to the spatial

95   variability of snow accumulation (snow blowing, terrain curvature) (Lehning et al., 2008), or

96   affect the energetic exchange between terrain and the snowpack (temperature, incoming solar

97   radiation), so the importance of topographic variables is modified during the season (Molotch

98   et al., 2005). In addition, during a snow season the terrain changes markedly (is smoothed) by

99   snow accumulation (Schirmer et al., 2011). However, few studies have systematically

100 analyzed the intra- and inter-annual persistence of the relation between snow distribution and

101 topography. Recent studies have assessed whether the influence of topography is constant

102 among different years; e.g. the similarities observed at the end of the accumulation season

103 (Schirmer and Lehning, 2011; Schirmer et al., 2011), or the consistent fractal dimensions in

104 two analyzed years (Deems et al., 2008); in both cases there was a relation with the dominant

105 wind direction, which highlights the predictive ability of topographic variables.

106 The main focus of this study was to assess the influence of topography on the spatial

107 distribution of snowpack and its evolution over time. The high temporal and spatial density of

108 the data set collected during the study enabled analysis of the main topographic factors

109 controlling snow distribution, and assessment of whether topographic control of the snowpack

110 varied during the snow season and between years having very contrasting climatic conditions.

111 For this purpose, we conducted 12 surveys over 2012 (6) and 2013 (6) in a small mountain

112 catchment representing a typical subalpine environment in the central Spanish Pyrenees, and

113 obtained high resolution SD measurements using LIDAR technology with a TLS.

114 **2. Study area and snow and climatic conditions**

115 The Izas experimental catchment (42°44′N, 0°25′W) is located in the central Spanish

116 Pyrenees (Fig. 1). The catchment is on the southern side of the Pyrenees, close to the main

117 divide (Spain–France border), in the headwaters of the Gallego River valley, and ranges in

118 elevation from 2000 to 2300 m above sea level. The catchment is predominantly east-facing,

119 with some areas facing north or south, and has a mean slope of 16°. There are no trees in the

120 study area, and the basin is mostly covered by subalpine grasslands dominated by Festuca

121 eskia and Nardus stricta, with rocky outcrops in the steeper areas. Flat, concave and convex

122 areas occur in the basin.

123 The climatic conditions are influenced by the proximity of the Atlantic Ocean, with the

124 winters being humid compared with zones of the Pyrenees more influenced by Mediterranean

125 conditions. The mean annual precipitation is 2000 mm, of which snow accounts for

126 approximately 50% (Anderton et al., 2004). The mean annual air temperature is 3 °C, and the

127 mean daily temperature is < 0 °C for an average of 130 days each year (del Barrio et al.,

128 1997). Snow covers a high percentage of the catchment from November to the end of May.

129 The two years analyzed in the study represent climatic extremes during recent decades.

130 Severe drought occurred during 2012, leading to snow accumulation well below the long-term

131 average. The thickness of the snowpack, measured at the automatic weather station (AWS,

132 Fig. 1), during winter in this year was less than the 25th percentile of the available historical

133 data series of this AWS (1996–2011) (Fig. 2). Only at the end of spring did late snowfall

134 events increase the amount of snow, but this rapidly melted. The opposite occurred in 2013, a

135 year in which the deepest snowpack and the longest snow season of recent decades were

136 recorded. Winter and spring in 2013 were extremely humid, with temperatures mostly

137 between the 25th and 75th percentiles of the AWS historical series. SD accumulation was

138 very high between February and June (exceeding the 75th percentile). In some areas of the

139 basin snow lasted until late July, which is one month longer than in most of the preceding

140 years for which records are available. Regarding net solar radiation data (short wave), no

141 measurements were available before December 2011, However the annual evolution has been

142 tracked on Figure 2 (bottom) showing a clear increase of incoming solar radiation while snow

143 season advance, with high variability due to meteorological factors.

3. Data and methods

3.1. Snow depth measurements

146 During the study period high resolution SD maps (Fig. 3) were generated using a long range

147 TLS (Riegl LPM-321), which enables safe acquisition of SD information with short

148 acquisition times from remote areas, compared with measurements obtained manually. This

149 technique has been extensively tested (Prokop et al., 2008; Revuelto et al., 2014; Schaffhauser

6

et al., 2008), and systematically applied to the study of snow distribution in mountain terrain (Egli et al., 2012; Grünewald et al., 2010; Mott et al., 2013; Schirmer et al., 2011). In a previous study the mean absolute error in the most distant areas of the catchment was less than 10 cm (Revuelto et al., 2014), which is consistent with errors reported in previous studies (Grünewald et al., 2010; Prokop, 2008; Prokop et al., 2008; Schaffauser et al., 2008).

TLS provides high resolution three dimensional information on the terrain. Nevertheless, error sources need to be considered because they can have large effects on the measurements. To reduce the influences of TLS instability (originated by small displacements of the tripod because TLS vibrations while it is operating), which leads to misalignment with reference points; and atmospheric change, a well-defined protocol must be applied. The protocol applied in this study for generating high resolution SD maps with a 1 m cell size was described by Revuelto et al., (2014). This protocol is based on the following main points: data collection; which includes experimental setup design and information acquisition by the scanning procedure; and data processing, when data is filtered, quality checked and the SD maps generated. Mainly, the methodology was based on differences between DEMs obtained with snow coverage in the study area and a DEM taken at 18 July 2012, when the catchment had no snow cover. Twelve SD maps at a spatial resolution of 5 m were generated for the 2012 and 2013 snow seasons (Fig. 3). In each year three surveys were undertaken from February to April (2012: 22 February, 2 April, 17 April; 2013: 17 February, 3 April, 25 April), and three were undertaken from May to June when dominated intense melting conditions (2012: 2, 14 and 24 May; 2013: 6, 12 and 20 June). The average SD and SCA, and the maximum SD are shown in Table 1. It shows that much lower SD and SCA were observed in 2012 compared to 2013.

3.2. Digital elevation model and topographic variables

From the two scan stations located in the study area (Fig. 1), 86% of the total area of the catchment was surveyed using the TLS. DEMs of 1 m grid size were initially obtained from

176 point clouds of varying density in different areas, but always with a minimum of 1 point/m^2

177 (Revuelto et al., 2014). Some of the predictor variables cannot be calculated where data gaps

178 occur in the DEM (e.g. the topographic position index), and others require a DEM with a

179 greater surface than the area scanned during the study (e.g. to calculate the potential solar

180 radiation, including the shadow effect from surrounding topography, or to calculate the

181 maximum upwind slope parameter, it is included topographic information for distances up to

182 1200 m from the exterior limit of the DEM obtained with the TLS). Thus, a DEM having a 5

183 m grid-size, available from the Geographical National Institute of Spain (Instituto Geográfico

184 Nacional, www.ign.es), was combined with the snow-free DEM obtained using the TLS

185 resampled from 1 m to 5 m resolution (the empty raster of the Geographical National Institute

186 was used for the resampling, averaging all values within each cell). The 1 m grid-size SD

187 maps were also resampled to 5 m to enable matching of the two different data sources.

188 To characterize the terrain characteristics, eight variables were derived from the final DEM,

189 including: (i) elevation (*Elevation* or *Elev.*), (ii) slope (*Slope*), (iii) curvature (*Curvature* or

190 *Curv.*), (iv) potential incoming solar radiation under clear sky conditions (*Radiation* or *Rad.*),

191 (v) easting exposure (*Easting* or *East.*), (vi) northing exposure (*Northing* or *North.*), (vii) the

192 topographic position index (*TPI*) and (viii) maximum upwind slope (*Sx*).

193 *Elevation* was obtained directly from the DEM, while the other variables were calculated

194 using ArcGIS10.1 software. This software calculates *Slope* as the maximum rate of change in

195 value from a specific cell to that of its neighbors (15 x 15 m window size), and *Curvature* is

196 determined from the second derivative of the fitted surface to the DEM in the direction of

197 maximum slope of the terrain for the neighbors cells (15 x 15 m window size too). *Radiation*

198 was obtained using the algorithm of Fu and Rich (2002) and reported in Wh/m^2 based on the

199 average conditions for the 15-day period prior to each snow survey. This algorithm calculates

200 the potential incoming solar radiation (short wave) under clear sky conditions, which may

201 strongly differ from the real radiation as a consequence of cloud cover. This measure provided

202 the relative difference in the extraterrestrial incoming shortwave solar radiation among areas

203 of the catchment for a given period under given topographical conditions (Fassnacht et al.,

204 2013). In this way, *Radiation* can be considered as a good proxy of the spatial distribution of

205 incoming solar energy within the study area. *Easting* and *Northing* exposure were calculated

206 directly as the sine and cosine, respectively, of the angle between direction north and terrain

207 orientation or aspect. It provided information on the east (positive)/west (negative) exposure

208 and the north (positive)/south (negative) exposure.

209 The *TPI* provides information on the relative position of a cell in relation to the surrounding

210 terrain at a specific spatial scale. Thus, this index compares the elevation of each cell with the

211 average cell elevation at specific radial distances as follows (De Reu et al., 2013; Weiss,

212 2001):

213 $$TPI = z_o - \bar{z} \qquad\qquad\qquad (1)$$

214 $$\bar{z} = \frac{1}{n_R}\sum_{i \in R} z_i \qquad\qquad\qquad (2)$$

215 Where z_o is the elevation of the cell in which *TPI* is calculated and $\bar{z}$ is the average elevation

216 of surrounding cells obtained from (2) for a radial distance *R*. For each pixel the *TPI* was

217 calculated for 5, 10, 15, 25, 50, 75, 100, 125, 150 and 200 m radial distances (scale factors).

218 For specific wind directions, the maximum upwind slope parameter, averaged for 45 ° upwind

219 windows ($\overline{Sx}$; Winstral et al., 2002) provided information on the exposure or sheltering of

220 individual cells at various distances, resulting from the topography. Rather than considering

221 the contribution for the dominant wind directions (Molotch et al., 2005), $\overline{Sx}$ (*Sx* further on)

222 values for eight directions were selected and directly related to the SD. The directions were:

223 0° for north (N), 45° for northeast (NE), 90° for east (E), 135° for southeast (SE), 180° for

224 south (S), 225° for southwest (SW), 270° for west (W), and 315° for northwest (NW). For *Sx*,

225 the searching distances (Winstral et al., 2002) considered were 100, 200, 300 and 500 m.

226 These distances were selected to enable assessment of the range at which *Sx* exhibited greatest

227 control on SD dynamics, as has occurred in previous studies (Schirmer et al., 2011; Winstral

228 et al., 2002).

3.3. Statistical analysis

230 The 12 SD maps at 5 m spatial resolution were related to each of the topographic variables

231 considered (including the 40 *Sx* combinations, and the 9 distances for *TPI*). The large number

232 of cells for which SD data were available enabled robust correlations between topography and

233 snow distribution to be obtained, and provided a very large data set for training and validating

234 the SD distribution models.

235 Pearson's r coefficients were obtained between SD and each topographic variable. Using the

236 whole data set, each variable was correlated, for all available points, with the SD value for the

237 specific survey day. Given the large amount of data for surveys, the degrees of freedom for

238 correlation analyses were very high and hence they can account for statistically significant

239 correlations even with very low correlation coefficients. Moreover, the use of a very dense

240 data set of observations may have associated problems derived from spatial autocorrelation

241 (Koenig, 1999). For reducing effects derived from spatial autocorrelation we followed a

242 Monte Carlo procedure, in which 1000 random samples of 100 SD cases were extracted from

243 the entire data set (an average of 20,000 SD measurements for each day) and correlated with

244 topographic variables for assessing significance. A threshold 95% confidence interval ($\alpha <$

245 0.05) was used to assess the significance of correlations (r = +/– 0.197, based on 100 cases).

246 The spatial scales of *Sx* and *TPI* for which SD showed a higher correlation; 200 m and 25 m

247 respectively, were selected for further analysis (not presented in the manuscript).

248 To assess the explanatory capacity when all topographic variables were considered

249 simultaneously, two statistical models were used: (1) multiple linear regressions (MLRs) and

250 (2) binary regression trees (BRTs). A wide variety of regression analyses for interpretation of

251 much more complex spatial data are available with greater capacity than MLRs and BRTs to

252 deal with spatial autocorrelation issues and the non-linear nature of the relationship between

253 predictors and the response variable (Beale et al., 2010). However, in this study we used

254 MLRs and BRTs because these methods have been and are still widely used in snow studies,

255 and because both enable to isolate accurately the weight of each independent variable within

256 the model, which was the main objective of this research, rather than deriving models with

257 maximum predictive capacity. Prior to run the models a principal component analysis (PCA)

258 was applied to the entire data set for detecting correlations between independent variables that

259 could originate multicolinearity in MLR and BRT. This analysis (not shown) grouped the

260 topographic variables in three components, showing that *TPI* and *Curvature* are highly

261 correlated with PCA component one, and also *Northing* and *Radiation* (but in this case with

262 opposite signs) presented high correlation with component two of the PCA. *TPI* and *Northing*

263 showed both higher correlations with their respective components and in general higher

264 Pearson's r coefficients with SD than *Curvature* and *Radiation* (see result section). Therefore

265 *Curvature* and *Radiation* were discarded as predictors in MLR and BRT analyses.

266 (1) *Multiple linear regression* estimates the linear influence of topographic variables on SD.

267   Despite its simplicity and the rather limited capability under nonlinear conditions (López-

268   Moreno et al., 2010), MLR was used to quantify the relative contribution of each variable

269   to the entire SD distribution model. SD was calculated from the topographic variables at

270   a specific location and day. The threshold for a variable to enter in the model was set at α

271   < 0.05. Beta coefficients (obtained dividing the standardized units of the coefficients by

272   the mean value of each variable) were used to compare the weight of each variable within

273   the regression models. As a first step, a reduced data set (1,000 cases) was randomly

274   extracted to avoid an excessive number of observations that may lead to spurious

275   identification of statistically significant predictor variables. A stepwise procedure was

276   used to obtain these variables from the random extraction. The variables determined for

277   each survey were used to obtain the final model, but using the entire data set (except

278   5,000 cases for model validation), forcing variables entrance in models.

279　　(2) *Binary regression trees* have been widely used to model snowpack distribution from

280　　　　topographic data (Erxleben et al., 2002; Molotch et al., 2005). These are nonparametric

281　　　　models that recursively split the data sample, based on the predictor variable that

282　　　　minimizes the square of the residuals obtained (Breiman, 1984). One BRT was created

283　　　　for each sampling date. The BRTs were run until a new split was not able to account for

284　　　　1% of the explained variance, or when a node had less than 500 cases; a maximum of 15

285　　　　terminal nodes was set to reduce tree complexity. As there were no over-fitting problems

286　　　　associated with sample size, 15,000 cases were used to grow the trees and 5,000 cases

287　　　　were used for validation. By scaling the explained variance of each variable introduced

288　　　　into each BRT (based on the % of the total explained variance by the BRT), we were able

289　　　　to compare the relative importance of each topographic variable between the different

290　　　　models.

291　Coefficients of determination (r^2) and Willmott's D statistic were used to assess the ability of

292　each model to predict SD over an independent random sample of 5,000 cases. Willmott´s D

293　was determined using equation (3) (Willmott, 1981):

294　$D = 1 - \frac{\sum_{i=1}^{N}(P_i - O_i)}{\sum_{i=1}^{N}(|P_i - \bar{O}| + |O_i - \bar{O}|)^2}$　　　　　　　　　　(3)

295　where N is the number of observations, O_i is the observed value, P_i is the predicted value, and

296　$\bar{O}$ is the mean of the observed values. The index ranges from 0 (minimum) to 1 (maximum

297　predictive ability).

298　**4. Results**

299　**4.1. Single correlations**

300　Table 2 shows the correlation between SD and *Sx* for the eight wind directions at a distance of

301　200 m (identified as the best correlated searching distance in previous analysis). Despite

302　differences in magnitude, the correlations for surveys carried out at the beginning of the

303　season (22 February 2012 and 17 February 2013) in each year showed that SD was clearly

affected by N and NW wind directions. The contribution of N and NW wind directions is
clearly evident for the surveys on 17 February 2013 (Figure 4, where wind roses with average
wind speeds and direction, for the 15 day period before each survey are presented), when
greater SD was recorded in the leeward slopes from a northerly direction (Fig. 3, northerly
areas of the maps). In the two years of the study a correlation with W and SW wind directions
was observed to increase progressively during the snow season (Fig. 4 and Table 2
correlations). In 2013 this phenomenon was less marked because of the greater SD
accumulation at the beginning of the snow season accompanied with NW direction winds,
which resulted in only moderate changes in the Sx for the most strongly correlated wind
directions. It was also observed that in both study years once the snow had started to melt (the
last three surveys in each season) the snow distribution did not change in relation to Sx
directions. The best correlated Sx directions for each survey are in good agreement with wind
roses main directions (Fig. 4). These directions for survey days are: 315º for 22 Feb. 2012,
270º for 02 and 17 April 2012 and 225º for the three surveys in May 2012; in 2013, 315º was
the best correlated direction for 17 Feb., and 270º for the other five surveys of the snow
season.

Correlations between the best correlated Sx direction for each day and SD were compared
with correlations between SD and the other topographic variables (Table 3). This showed that
Sx had one of the greatest coefficient of correlation with SD (range 0.22–0.56). The
correlations were higher during the accumulation periods, especially in the 2013 snow season,
with a reduction in correlations values occurring during the melt period at the end of each
snow season.

The TPI at 25 m showed the highest correlation with SD for the 12 sampled days. During
2012 the mean correlation values ranged from –0.32 to –0.58 for those surveys during which
snow accumulation dominated in the days preceding the surveys. The r values were closer to
the significance level for the surveys where the preceding days were dominated by melting

330   conditions (14 and 24 May). In 2013, the *TPI* was more highly correlated with SD than in

331   2012, with Pearson's r coefficients < -0.6 for all survey days. *Curvature* also had a high

332   correlation with SD, and similar to *TPI* with a 25 m searching distance was significantly

333   correlated on all the survey dates, but unlike the *TPI,* the correlation of *Curvature* with SD did

334   not decrease during the snowmelt periods. The significant correlations of *TPI* and *Curvature*

335   with SD highlight the importance of terrain curvature on the SD distribution. The importance

336   of terrain curvature at different scales for SD distribution is clearly evident in Figure 3, which

337   shows that higher SD values were usually found for concave areas, which showed snow

338   presence until the end of each snow season.

339   The correlation between *Elevation* and SD varied among survey days (Table 3). The

340   correlations were usually positive, but only statistically significant (or approaching

341   significance) for days when melting dominated (the last two surveys in 2012 and 2013). *Slope*

342   was relatively weakly correlated with SD during the 2012 snow season. In 2013 the

343   correlation was greater, and was statistically significant for all days. Similarly to *Elevation*,

344   the correlation between *Slope* and SD was variable between the two study years, and showed

345   a similar temporal pattern to *Easting*, probably because of the presence of steeper areas on the

346   east-facing slopes.

347   The correlation between *Northing* and SD was rarely statistically significant, highly variable

348   and contributed to explaining SD in a very different ways in 2012 and 2013. In 2012 no

349   correlation between SD and *Northing* was found during the accumulation period, but during

350   the melting period a slight positive correlation was observed, as snow remained longer on

351   north-facing slopes. The 2013 snow season started with a large precipitation event dominated

352   by strong winds from a northerly direction, leading to high levels of snow accumulation on

353   the south-facing slopes. This explains the strong and statistically significant negative

354   correlation of SD with *Northing* for 17 February 2013. This event influenced the rest of the

355   season (as evident in Table 2 for 2013), but a progressive decrease in its influence was

356 evident for the following survey days. *Radiation* had an almost opposite influence on SD to

357 that observed for *Northing*. During the melting period, for each year, the Pearson's r

358 correlation between SD and *Radiation* was negative, indicating a thinner snowpack on the

359 most irradiated slopes. This relation was statistically significant at the end of the 2013 snow

360 season. However, during the accumulation period in 2013 statistically significant and positive

361 correlations were observed with *Northing* and *Radiation*, which are connected to the strong

362 snow redistribution by winds from N-NW directions.

363 **4.2. Multiple Linear Regression and Binary Regression Tree models**

364 Figure 5 shows the Willmott's D values and the coefficients of determination (r^2) obtained in

365 the comparison of observed and predicted values using MLRs and BRTs for a data set

366 reserved for validation (5000 cases). The MLRs produced r^2 values ranging from 0.25 to 0.65

367 and Willmott's D values ranging from 0.60 to 0.88, while the BRTs produced r^2 values

368 ranging from 0.39 to 0.58 and Willmott´s D values ranging from 0.72 and 0.85. For both

369 methods the relations between the observed and predicted values was stronger for 2013.

370 Accuracy decreased at the end of the snow season, when the snowpack was mostly patchy

371 across the basin; this was particularly the case for the end of the 2012 season. Overall, the

372 performance of the MLRs was more variable than that of the BRTs, which were more

373 constant amongst the various snow surveys. For those days on which the models were most

374 accurate in predicting SD variability, the MLRs showed slightly better scores than the BRTs.

375 However, for days on which the accuracy between predictions and observations was lower,

376 the BRTs provided better estimates than the MLRs. For 2012, slightly better results were

377 obtained using MLRs, while the opposite occurred in 2013. Nevertheless, only large

378 differences in the accuracy of each model were evident by the end of 2012 snow season, in

379 the two last surveys, which were characterized by thin and patchy snowpack.

380 As shown for single correlations, the *TPI* variable explained most of the variance in MLR

381 models developed for all analyzed days (Table 4). The contribution of the other variables

15

382 varied markedly among surveys, particularly when the two years were compared. In most

383 cases, *Elevation* was the second most important variable explaining the SD distribution in

384 2012, followed by *Sx* and *Slope*. The other variables made a much smaller contribution, or

385 were not included in the models. The contribution of *Elevation* was much less in 2013, and it

386 was not included in three of the six surveys, whereas in 2012 it was included in all surveys.

387 For the entire 2013, *Sx* was the second most important variable, followed by *Easting*, which

388 had an almost negligible influence in 2012. *Northing* was only included in the models for the

389 surveys carried out during periods dominated by snow accumulation, and was not included in

390 the models during the periods dominated by melting.

391 Figure 6 shows two examples of BRTs, obtained for the days 2 May 2012 (upper panel) and 3

392 April 2013 (bottom panel), which accounted for the largest amount of snow accumulation in

393 both years. The variable *TPI* determined the first branching point, and this occurred in the

394 majority of the trees obtained (not shown). After the first branching, other variables were

395 significant in the model, including *Sx* and *TPI* for 2 May 2012,and *Sx* and *Northing* for 3

396 April 2013, demonstrating the importance of these variables in the subsequent branching of

397 the trees.

398 The relative importance (scaled from 0 to 100) of each topographic variable in each BRT is

399 shown in Table 5. This shows that *TPI* was the first most important variable explaining SD

400 for all survey days. For the 2012 snow season, *TPI* explained more than 67% of the total

401 explained variance in all BRTs, and 75% during the accumulation period (the first three

402 surveys). Thus, for most of the survey days the variance explained by the other variables was

403 < 30%. Besides *TPI* was in all cases the first split variable (which accounted from a 23 to a

404 30% of the explained variance), with a critical value that ranged from -0.67 m to -0.43 m and

405 an average value of -0.54 m. The second most important variable explaining the SD

406 distribution in 2012 differed amongst survey days. Thus, *Sx* was the second most influential

407 variable during May (except for 24 May 2012), following the largest snowfall in the season

(which occurred the 1 May 2012), and *Elevation* was the most important variable in the other

surveys during 2012. *Northing* also had an evident influence during the two first surveys of

the year, but subsequently had minimal explanatory capacity, as was the case for all the other

variables. In 2013 *TPI* was also the main contributor to the total explained variance,

exceeding 50% for almost all survey days, and approaching or > 70% during the snowmelt

period. For this year, also *TPI* was the first split variable in nearly all BRT, with critical

values ranging from -0.47 m to -0.15 m and an average value of -0.28 m; except for the 13

Feb. 2013, in which *Sx* was the first split variable. The influence of *Sx* was more important in

2013 than in the previous year. At the beginning of 2013 the contribution of *Sx* to the total

explained variance was almost 46%, and remained > 20% for the rest of the snow season. An

exception was the last survey, when melting dominated and its effect declined to 12%. When

snow was not mobilized for long periods by wind (no changes on the best correlated wind

direction of *Sx* are observed), the SD distribution was more dependent on variables related to

terrain curvature (*TPI* and *Curvature*). During 2013, *Elevation* contributed approximately 5%

to the total explained variance during the entire snow season. *Northing* made a significant

contribution to the model (14.7%) only one day (3 April 2013), and a smaller contribution on

the following survey day (25 April 2013). When included in the BRTs, the other variables

(*Easting*, *Radiation*) made minor contributions to the total explained variance.

Figure 7 shows the mean contribution of each topographic variable versus the coefficient of

variation from the twelve surveys for the different statistical approaches considered in this

study (Pearson´s r coefficients, beta coefficients of the MLRs and the contribution to the

explained variance for each BRT). Clearly, *TPI* is the most important variable to explain the

snow distribution in the catchment, but it is also the variable that exhibits a lower variability

between the different surveys (CV<0.2). Besides it has been introduced as predictor for MLRs

and BRTs in all studied days. *Sx* is the next variable in importance to explain snow

distribution, being introduced as predictor in the majority of the modelled days (11 and 10 out

of 12 days for MLRs and BRTs respectively). It shows a low temporal variability when correlation´s coefficients are calculated (CV=0.24), but the variability in its contribution to MLRs and BRTs increases noticeably, with CV values of 0.35 and 0.59 respectively. The rest of the variables show a much lower mean contribution for explaining snow distribution and a high temporal variability in their explanatory role. Lower CV values are observed for MLRs, ranging the majority between 0.3 and 0.4, than for BRTs models, ranging the majority between 0.4 and 0.8.

5. Discussion

The distribution of snow in mountain areas is highly variable in space and time, as shown for Izas experimental catchment during two consecutive years. Many meteorological and topographic parameters affect the snow distribution and its evolution through time with different weights subjected to several factors. In this context, we demonstrated that terrain characteristics significantly affect SD distribution in a subalpine catchment. Also we have showed that its effect evolved during the snow accumulation and melting periods over two years having highly contrasting climatic conditions and snow accumulation amounts

Many studies have analyzed the spatial distribution of SD in mountain areas considering both, intra- and inter- annual variability of the topographic control on the snowpack distribution (Anderton et al., 2004; Erickson et al., 2005; López-Moreno et al., 2010; McCreight et al., 2012). Other researches have also focused their attention in long-term inter-annual snow distribution analyses (Jepsen et al., 2012; Sturm and Wagner, 2010; Winstral and Marks, 2014). The results of these previous works have highlighted the difficulties in fully explaining the distribution of snow in complex mountainous terrain. In addition, results differ among studies, and suggest that different variables govern the distribution of snowpack among areas as consequence of their different characteristics and geographical settings. These differences include surface extension, the altitudinal gradients, the importance of wind redistribution, the

presence or absence of vegetation and the topographic complexity as concluded by Grünewald et al., (2013) in a study where seven study sites across the world were considered. Most of the topographic variables investigated in this study have been included in previous studies, including *Elevation, Slope, Radiation, Curvature* and *Sx*. Other variables, in particular *TPI*, have received little attention in previous research (López-Moreno et al., 2010). We showed that *TPI* at a scale of 25 m had the greatest capacity to explain the SD distribution in the study catchment. *Curvature* (which refers to a smaller spatial scale of terrain curvature when compared with *TPI*) is also highly correlated with the SD distribution, but not as much as *TPI*. This reinforces the importance of considering terrain curvature at various scales for explaining the SD distribution in mountain environments. The correlation between snowpack and the *TPI* decreased during melting periods, whereas the correlation with *Curvature* remained constant. This suggests that snow accumulates more in small deep concavities, but is shallower at the end of the season in wider concave areas that were identified by the 25 m *TPI* scale. This effect was evident at the end of the snow season, when snow was present only in deep concavities, as shown in Figure 3. To explain the snow distribution, Anderton et al. (2004) compared the relative elevation of a cell with the terrain over a 40 m radius, and observed that this had a major role on SD distribution, what sustain curvature importance at different scales.

The maximum upwind slope (*Sx*; Winstral et al., 2002) has also been identified as a key variable explaining snow distribution, improving the results obtained when it is introduced into models. Our results, 200 m searching distance for *Sx*, is comparable with those of other studies that have shown that the optimum searching distance for correlating *Sx* with the SD distribution is 300 m (Schirmer et al., 2011), which is not a large difference for the considered distances in this work reaching 500 m. As it is observed from the reported wind information, Izas experimental catchment has W-NW dominant wind direction what is consistent with the best correlated *Sx* directions. For this reason, the *Sx* preferred direction for each date was

selected, and showed that there were intra-annual shifts in the most highly correlated direction. The change in the most important *Sx* direction was similar between the 2012 and 2013 snow seasons; it started with a northerly component and evolved to a dominant westerly direction. We also found a decrease in the correlation between *Sx* and the snow distribution at the end of each snow season, when melting conditions dominated. This is consistent with the findings of previous studies (Winstral and Marks, 2002).

Sx parameter takes into account sheltering effects with topographic origin in relation to wind directions. SD distribution maps show higher SD amounts in leeward slopes, located in E-SE slopes. *TPI* is not able to explain snow drifts, because this index considers the topographic characteristics in all directions. Nevertheless, terrain characteristics at the study site in relation to SD distribution have shown a higher importance of *TPI* when compared to *Sx*. The most plausible explanation accounting for this result is that the basin has a rather reduced size, shows the same general aspect (SE facing) and topography is relatively gentle. Under such conditions, during wind blowing events snow is accumulated in all wide concavities of the basin (represented by *TPI*) independently of its specific location. Nonetheless, wind redistribution will be affected by a combination of local topography and main wind directions; which makes necessary to consider the *Sx* parameter. As it has been observed, this effect lasts in time until the melting season is advanced.

Only for two days (22 February 2012 and 2 April 2012) there was no contribution (or it was minor) of *Sx* to explain SD distribution, according to BRTs and MLRs. On these days *Northing* was introduced into the models, and was found to explain some of the variance of *Sx* from northerly direction, the best correlated direction for these days (Table 2).

Although *Elevation* has been found to largely explain the snow distribution in areas having marked altitudinal differences (Elder et al., 1998; Erxleben et al., 2002; Molotch and Bales, 2005), in our study no strong association was found between SD and *Elevation*, with significant correlations occurring only during the snowmelt period. This is because of the low

elevation range of the study area (300 m). During the accumulation period the entire

catchment is generally above the freezing height. However, during spring the 0°C isotherm

shifts to higher elevations, which may lead to different melting rates within the basin. Despite

the relatively weak correlation between *Elevation* and SD, this variable was introduced as a

predictor in the MLRs and BRTs for most of the days analyzed. Similarly, López-Moreno et

al. (2010) reported that elevation was of increasing importance as the grid size increased.

Anderton et al. (2004) also informed about the importance of elevation to explain snowpack

distribution in the same study area. The results of the present study suggest the increase in

importance of *Elevation* at the end of the snow season, and particularly when it is considered

in combination with other topographic variables in MLR and BRT models.

Slope has a weak explanatory capacity for snow distribution, probably because the slope in

most of the catchment is not steep enough to trigger gravitational movements including

avalanches and slushes during the snowmelt period, which could thin the snowpack on the

steepest slopes (Elder et al., 1998). Most likely, some of *Slope* explanatory capacity is

included on *Radiation* explanatory capacity, because it affects solar light incident angle,

besides the steeper areas of the catchment are in south facing zones. Nevertheless quantifying

such kind of effects is highly difficult due to the high complexity of SD dynamic in mountain

terrain.

Radiation, *Northing* and *Easting* showed no close correlation with the snowpack distribution;

their relationships with SD were variable over time, with statistically significant correlations

occurring on some days and only weak correlations on other days. The results suggested that

Radiation and *Northing* (which showed almost opposite patterns) may be related to SD for

two different reasons. During the accumulation period in 2013 heavy snowfalls associated

with northerly winds led to the accumulation of deep snow on south-facing areas (more

irradiated), whereas during the snowmelt period the greater exposure of the southern slopes to

solar energy led to a positive (negative) correlation with *Northing* (*Radiation*). This

537 phenomenon was also observed by López-Moreno et al. (2013), using a physically-based

538 snow energy balance model in the same study area. Moreover, the high and opposite

539 correlation between *Northing* and *Radiation* obtained in PCA results (not shown in the

540 manuscript), was showing a potential problem of multicollinearity. Thus, only *Northing* was

541 considered for MLRs and BRTs (the same occurred with *TPI* and *Curvature*, being only

542 considered in statistical models the *TPI*). Although *Northing* did not show a significant

543 correlation with SD during accumulation periods; when the surveys were closer to the

544 snowmelt period, the negative correlation of this variable with SD was more evident, possibly

545 due to the increase of the difference in the energetic exchange between sun exposed and

546 shaded areas. The importance of *Northing* in MLR models, combined with the contribution of

547 *Easting* during the accumulation period may be related to the high snow redistribution

548 originated by wind directions from N- NW directions. Therefore terrain aspect relation with

549 SD distribution (considered with *Northing* and *Easting*) in winter is tightly related to the

550 accumulation patterns resulting from wind redistribution, whereas in spring they were

551 associated with the unequal distribution of solar radiation, which leads to higher melting rates

552 on the most irradiated slopes, what has shown better explanatory capacity than *Radiation* at

553 Izas Experimental catchment.

554 The MLRs and BRTs provided reasonably high accuracy scores when observed and predicted

555 SD data were compared. The scores were comparable, and in some cases better, to values

556 reported in previous researches using similar methods. As an example, Molotch et al., (2005)

557 reported r^2 values between 0.31 and 0.39 using BRT; and Winstral et al., (2002), who

558 considered different number of terminal nodes of BRT, obtained an optimal tree size of 16

559 nodes data set with an r^2 value close to 0.4. Moreover results presented here were obtained

560 from a separate data set, and data used to create the models were not considered for testing,

561 thanks to the large available data set. One reason for the improvement may be the use of the

562 *TPI* as a SD predictor, as this variable has not been considered in previous studies.

563   Nevertheless, it should be noted that the study sites considered in other studies, could differ in

564   terms on complexity of terrain, and also in SD accumulation amounts. For the 12 survey days

565   the *TPI* had the greatest explanatory capacity in both approaches. However, based on

566   comparison of the different dates and surveys, the other variables made more varying

567   contributions, as a result of the different roles they play during the snow accumulation and

568   melting periods, and the wind conditions during the main snowfall events. The models had

569   less capacity to explain spatial variability of the snowpack when the snow was thinner and

570   patchy. The BRT and MLR approaches were consistent with respect to error estimates. The

571   results obtained using each approach were comparable, so the trends in the variable ranking

572   with both models for each survey day were similar. Only during conditions of snow scarcity

573   did the BRT approach demonstrate better capability to relate SD to topography. This is

574   probably a consequence of the greater capacity of BRTs to take account of the nonlinear

575   response of the snowpack to topography, and the occurrence of sharp thresholds typical of

576   days when the snowpack is patchy (López-Moreno et al., 2010; Molotch et al., 2005).

577   Despite model results differ between survey days and years, the most important variable, *TPI*,

578   is always present in the models and their contribution to the total explained variances show

579   very low CV values. Other variables with an also important role to explain SD distribution

580   (i.e. *Sx*) are included in most of the models as predictors showing their influence on snowpack

581   distribution, although their contribution to the final models changes noticeably amongst

582   different surveys. Moreover for 2012 and 2013 a consistent inter-annual distribution of the

583   snowpack in the catchment is observed; the areas of maximum SD and the location of snow

584   free zones were consistent between both years of the study, and more importantly there is a

585   strong consistency of the effect of topography on SD. This spatial consistency of snowpack

586   has implications for soil dynamics and plant cycles, because some parts of the basin will tend

587   to remain free of snow cover during longer periods favoring the presence of temporary frozen

588   soils, and reducing the isolation effect of snowpack to the plants (Keller et al., 2000; Pomeroy

589 and Gray, 1995). Besides, it suggests that the information acquired from TLS during several

590 years could be useful to design long-term monitoring strategies of SD in the basin based on

591 few manual measurements in representative points according their terrain characteristics.

6. Conclusions

593 The *TPI* at a 25 m searching distance was the best topographic variable, and the most

594 persistent in time, for explaining SD distribution in the Izas experimental catchment. This

595 suggests the importance of including this index in future snow studies, and the need to

596 establish the best searching distance for relating this variable to SD distribution at other study

597 sites. The maximum upwind slope (*Sx*) at a searching distance of 200 m was also an important

598 variable explaining the SD distribution, but its influence varied markedly between years and

599 surveys, depending of the specific wind conditions during and after main snowfall events.

600 Nevertheless, *Sx* has shown a similar evolution pattern for the best correlated direction in the

601 two analyzed snow seasons. The influence of the other topographical variables on the spatial

602 distribution of SD was lower, and showed higher intra- and inter-annual variability. The total

603 variance explained by BRTs and MLRs clearly decreased for periods on which the snowpack

604 was thinner and more patchily. The results from BRTs and MLRs models were consistent in

605 terms of variables importance ranking, and the explanatory capacities of the main variables

606 were similar for all surveys. Except *TPI*, that showed very low coefficient of variations for the

607 two approaches, the variability of the contribution of each topographic variable for the

608 different surveys was noticeably lower for MLRs than for BRTs.

7. Acknowledgments

8. References

Anderton, S.P., White, S.M., and Alvera, B.: Evaluation of spatial variability in snow water equivalent for a high mountain catchment. Hydrol. Process., 18, 435–453. 2004.

Bales, R.C., and Harrington, R.F.: Recent progress in snow hydrology. Reviews of Geophysics Supplement, 33, 1011–1020. 1995.

Barnett, T.P., Adam, J.C., and Lettenmaier, D.P.: Potential impacts of a warming climate on water availability in snow-dominated regions. Nature, 438, 303–309. 2005.

Del Barrio, G., Alvera, B., Puigdefabregas, J., and Diez, C.: Response of high mountain landscape to topographic variables: Central pyrenees. Landscape Ecol., 12, 95–115. 1997.

Beale, C.M., Lennon, J.J., Yearsley, J.M., Brewer, M.J., and Elston, D.A.: Regression analysis of spatial data. Ecol. Lett., 13, 246–264. 2010.

Beniston, M.: Climatic Change in Mountain Regions: A Review of Possible Impacts. Climatic Change, 59, 5–31. 2003.

639 Breiman, L.: Classification and regression trees. Wadsworth International Group, Belmont

640 (California) USA. 1984.

641 Caballero, Y., Voirin-Morel, S., Habets, F., Noilhan, J., LeMoigne, P., Lehenaff, A., and

642 Boone, A.: Hydrological sensitivity of the Adour-Garonne river basin to climate change.

643 Water Resour., Res. 43, W07448, DOI: 10.1029/2005WR004192. 2007.

644 Deems, J.S., Fassnacht, S.R., and Elder, K.J.: Fractal Distribution of Snow Depth from Lidar

645 Data. J. Hydrometeorol., 7, 285–297. 2006

646 De Rue, J., Bourgeois, J., Bats, M., Zwertvaegher, A., Gelorini, V., De Smedt., P.M., Chu,

647 W., Antrop., M., De Maeyer, P., Finke., P., Mairvanne, M.V., Verniers., J. and Crombé., P.:

648 Application of the topographic position index to heterogeneous landscapes. Geomorphology.

649 186 , 39-49. 2013.

650 Deems, J.S., Fassnacht, S.R., and Elder, K.J.: Interannual Consistency in Fractal Snow Depth

651 Patterns at Two Colorado Mountain Sites. J. Hydrometeorol. 9, 977–988. 2008

652 Egli, L., Jonas, T., Grünewald, T., Schirmer, M., and Burlando, P.: Dynamics of snow

653 ablation in a small Alpine catchment observed by repeated terrestrial laser scans. Hydrol.

654 Process., 26, 1574–1585. 2012.

655 Elder, K., Dozier, J., and Michaelsen, J.: Snow accumulation and distribution in an Alpine

656 Watershed. Water Resour. Res., 27, 1541–1552. 1991.

657 Elder, K., Rosenthal, W., and Davis, R.E.: Estimating the spatial distribution of snow water

658 equivalence in a montane watershed. Hydrol. Process. 12, 1793–1808. 1998.

659 Erickson, T.A., Williams, M.W., and Winstral, A.: Persistence of topographic controls on the

660 spatial distribution of snow in rugged mountain terrain, Colorado, United States. Water

661 Resour. Res., 41 (4), 1–17. 2005.

662 Erxleben, J., Elder, K., and Davis, R.: Comparison of spatial interpolation methods for

663 estimating snow distribution in the Colorado Rocky Mountains. Hydrol. Process., 16, 3627–

664 3649. 2002.

665   Fassnacht, S.R., and Deems, J.S.: Measurement sampling and scaling for deep montane snow

666   depth data. Hydrol. Process., 20, 829–838. 2006.

667   Fassnacht, S.R., Dressler, K.A., and Bales, R.C.: Snow water equivalent interpolation for the

668   Colorado River Basin from snow telemetry (SNOTEL) data. Water Resour. Res., 39 (8),

669   SWC31–SWC310. 2003.

670   Fassnacht, S.R., López-Moreno, J.I., Toro, M., and Hultstrand, D.M.: Mapping snow cover

671   and snow depth across the Lake Limnopolar watershed on Byers Peninsula, Livingston Island,

672   Maritime Antarctica. Antarct. Sci,. 25, 157–166. 2013.

673   Fu, P., and Rich, P.M.: A geometric solar radiation model with applications in agriculture and

674   forestry. Computers and Electronics in Agriculture, 37, 25–35. 2002.

675   Groffman, P.M., Driscoll, C.T., Fahey, T.J., Hardy, J.P., Fitzhugh, R.D., and Tierney, G.L.:

676   Colder soils in a warmer world: A snow manipulation study in a northern hardwood forest

677   ecosystem. Biogeochemistry, 56, 135–150. 2001.

678   Grünewald, T., Schirmer, M., Mott, R., and Lehning, M. Spatial and temporal variability of

679   snow depth and ablation rates in a small mountain catchment. The Cryosphere, 4, 215–225.

680   2010.

681   Grünewald, T., Stötter, J., Pomeroy, J.W., Dadic, R., Moreno Baños, I., Marturià, J., Spross,

682   M., Hopkinson, C., Burlando, P., and Lehning, M.: Statistical modelling of the snow depth

683   distribution in open alpine terrain. Hydrol. Earth Syst. Sci., 17, 3005–3021. 2013

684   Hosang, J., and Dettwiler, K.: Evaluation of a water equivalent of snow cover map in a small

685   catchment area using a geostatistical approach. Hydrol. Process., 5, 283–290. 1991.

686   Jepsen, S.M., Molotch, N.P., Williams, M.W., Rittger, K.E., and Sickman, J.O.: Interannual

687   variability of snowmelt in the Sierra Nevada and Rocky Mountains, United States: Examples

688   from two alpine watersheds. Water Resour. Res. 48, W02529. 2012.

Jost, G., Weiler, M., Gluns, D.R., and Alila, Y.: The influence of forest and topography on snow accumulation and melt at the watershed-scale. Journal of Hydrology, 347, 101–115. 2007.

Keller, F., Kienast, F., and Beniston, M.: Evidence of response of vegetation to environmental change on high-elevation sites in the Swiss Alps. Reg. Environ. Change, 1, 70–77. 2002.

Koenig, W.D.: Spatial autocorrelation of ecological phenomena. Tends in Ecology & Evolution, 14, 1 22-26. 1999.

Lehning, M., Löwe, H., Ryser, M., and Raderschall, N.: Inhomogeneous precipitation distribution and snow transport in steep terrain. Water Resour. Res., 44, W07404, DOI: 10.1029/2007WR006545. 2008.

Lehning, M., Grünewald, T., and Schirmer, M.: Mountain snow distribution governed by an altitudinal gradient and terrain roughness. Geophysical Research Letters 38. 2011.

Liston, G.E.: Interrelationships among Snow Distribution, Snowmelt, and Snow Cover Depletion: Implications for Atmospheric, Hydrologic, and Ecologic Modeling. J. Appl. Meteorol., 38, 1474–1487. 1999.

López-Moreno, J.I., and Nogués-Bravo, D.: A generalized additive model for the spatial distribution of snowpack in the Spanish Pyrenees. Hydrol. Process., 19, 3167–3176. 2005.

López-Moreno, J.I., Latron, J., and Lehmann, A.: Effects of sample and grid size on the accuracy and stability of regression-based snow interpolation methods. Hydrol. Process., 24, 1914–1928. 2010.

López-Moreno, J.I., Vicente-Serrano, S.M., Morán-Tejeda, E., Lorenzo-Lacruz, J., Kenawy, A., and Beniston, M.: Effects of the North Atlantic Oscillation (NAO) on combined temperature and precipitation winter modes in the Mediterranean mountains: Observed relationships and projections for the 21st century. Global Planet. Change, 77, 62–76. 2011.

713 López-Moreno, J.I., Fassnacht, S.R., Heath, J.T., Musselman, K.N., Revuelto, J., Latron, J.,

714 Morán-Tejeda, E., and Jonas, T.: Small scale spatial variability of snow density and depth

715 over complex alpine terrain: Implications for estimating snow water equivalent. Adv. Water

716 Resour., 55, 40–52. 2012a.

717 López-Moreno, J.I., Pomeroy, J.W., Revuelto, J., and Vicente-Serrano, S.M.: Response of

718 snow processes to climate change: spatial variability in a small basin in the Spanish Pyrenees.

719 Hydrol. Process., 27, 2637–2650. 2012b.

720 McCreight, J.L., Slater, A.G., Marshall, H.P., and Rajagopalan, B.: Inference and uncertainty

721 of snow depth spatial distribution at the kilometre scale in the Colorado Rocky Mountains:

722 The effects of sample size, random sampling, predictor quality, and validation procedures.

723 Hydrol. Process., 28, 933–957. 2014.

724 Molotch, N.P., and Bales, R.C.: Scaling snow observations from the point to the grid element:

725 Implications for observation network design. Water Resour. Res., 41, W11421, DOI:

726 10.1029/2005WR004229. 2005.

727 Molotch, N.P., Colee, M.T., Bales, R.C., and Dozier, J.: Estimating the spatial distribution of

728 snow water equivalent in an alpine basin using binary regression tree models: the impact of

729 digital elevation data and independent variable selection. Hydrol. Process., 19, 1459–1479.

730 2005.

731 Mott, R., Schirmer, M., Bavay, M., Grünewald, T., and Lehning, M.: Understanding snow-

732 transport processes shaping the mountain snow-cover. The Cryosphere, 4, 545–559. 2010.

733 Mott, R., Schirmer, M., and Lehning, M.: Scaling properties of wind and snow depth

734 distribution in an Alpine catchment. J. Geophy. Res.-Atmos., 116, D06106,

735 DOI:10.1029/2010JD014886. 2011.

736 Mott, R., Gromke, C., Grünewald, T., and Lehning, M.: Relative importance of advective heat

737 transport and boundary layer decoupling in the melt dynamics of a patchy snow cover.

738 Advances in Water Resources 55, 88–97. 2013.

739 Pomeroy, J.W., and Gray, D.M.: Snowcover accumulation, relocation, and management.

740 National Hydrology Research Institute, Saskatoon, Sask., Canada. 1995.

741 Pomeroy, J., Essery, R., and Toth, B.. Implications of spatial distributions of snow mass and

742 melt rate for snow-cover depletion: observations in a subarctic mountain catchment. Ann.

743 Glaciol., 38, 195–201. 2004.

744 Prokop, A.: Assessing the applicability of terrestrial laser scanning for spatial snow depth

745 measurements. Cold Reg. Sci. .Technol., 54, 155–163. 2008.

746 Prokop, A., Schirmer, M., Rub, M., Lehning, M., and Stocker, M., A comparison of

747 measurement methods: terrestrial laser scanning, tachymetry and snow probing for the

748 determination of the spatial snow-depth distribution on slopes. Ann. Glaciol., 49, 210–216.

749 2008.

750 Revuelto, J., López-Moreno, J.I., Azorin-Molina, C., Zabalza, J., Arguedas, G., and Vicente-

751 Serrano, S.M.: Mapping the annual evolution of snow depth in a small catchment in the

752 Pyrenees using the long-range terrestrial laser scanning. Journal of Maps, Volume 10, Issue 3,

753 2014, Pages 379-393. 2014.

754 Schaffhauser, A., Adams, M., Fromm, R., Jörg, P., Luzi, G., Noferini, L., and Sailer, R.:

755 Remote sensing based retrieval of snow cover properties. Cold Reg. Sci. .Technol., 54, 164–

756 175. 2008.

757 Schirmer, M., and Lehning, M.: Persistence in intra-annual snow depth distribution: 2. Fractal

758 analysis of snow depth development. Water Resour. Res., 47, W0951, DOI:

759 10.1029/2010WR009429. 2011.

760 Schirmer, M., Wirz, V., Clifton, A., and Lehning, M.: Persistence in intra-annual snow depth

761 distribution: 1.Measurements and topographic control. Water Resour. Res., 47, W09516,

762 DOI: 10.1029/2010WR009426. 2011.

763 Scipión, D.E., Mott, R., Lehning, M., Schneebeli, M., and Berne, A.: Seasonal small-scale

764 spatial variability in alpine snowfall and snow accumulation. Water Resour. Res., 49, 1446–

765 145. 2013.

766 Steger, C., Kotlarski, S., Jonas, T., and Schär, C.: Alpine snow cover in a changing climate: a

767 regional climate model perspective. Clim. Dynam., Volume 41, Issue 3-4 , pp 735-754. 2012.

768 Sturm, M., and Wagner, A.M.: Using repeated patterns in snow distribution modeling: An

769 Arctic example. Water Resources Research 46. 2010.

770 Trujillo, E., Ramírez, J.A., and Elder, K.J.: Topographic, meteorologic, and canopy controls

771 on the scaling characteristics of the spatial distribution of snow depth fields. Water Resour.

772 Res., 43, W07409, DOI:10.1029/2006WR005317. 2007.

773 Watson, F.G.R., Anderson, T.N., Newman, W.B., Alexander, S.E., and Garrott, R.A.:

774 Optimal sampling schemes for estimating mean snow water equivalents in stratified

775 heterogeneous landscapes. Journal of Hydrology 328, 432–452. 2006.

776 Weiss, A.D.: Topographic position and landforms analysis. ESRI user conference, San Diego

777 USA. 2001.

778 Willmott, C.J. On the Validation of Models. Phys. Geogr., 2, 184–194. 1981.

779 Winstral, A., and Marks, D.: Simulating wind fields and snow redistribution using terrain-

780 based parameters to model snow accumulation and melt over a semi-arid mountain

781 catchment. Hydrol. Process., 16, 3585–3603. 2002.

782 Winstral, A., Elder, K., and Davis, R.E.: Spatial Snow Modeling of Wind-Redistributed Snow

783 Using Terrain-Based Parameters. Journal of Hydrometeorol., 3, 524–538. 2002.

784 Winstral, A., and Marks, D.: Long-term snow distribution observations in a mountain

785 catchment: Assessing variability, time stability, and the representativeness of an index site.

786 Water Resour. Res. 50, 293–305. 2014.

787 Wipf, S., Stoeckli, V., and Bebi, P.: Winter climate change in alpine tundra: plant responses

788 to changes in snow depth and snowmelt timing. Climatic Change, 94, 105–121. 2009.

789 **9. Tables**

	Snow season 2012						Snow season 2013					
	22/02	02/04	17/04	02/05	14/05	24/05	17/02	03/04	25/04	06/06	12/06	20/06
Mean SD (m)	0.72	0.58	0.60	0.97	0.71	0.70	2.98	3.22	2.53	2.28	2.09	1.61
Max SD (m)	5.5	3.8	5.3	6.1	4.4	4.3	10.9	11.2	10.1	9.6	8.9	7.9
SCA (%)	67.2	33.5	94.1	98.8	30.9	18.9	98.8	100.0	96.3	86.4	77.1	67.0

790

791 **Table 1:** Summary statistics of the snowpack distribution and the snow covered area of the

792 basin. Note that snow covered area is expressed as a % of the total area surveyed by the TLS,

793 and the mean SD is the average of all SDs not including zero values.

794

	Snow season 2012						Snow season 2013					
	22/02	02/04	17/04	02/05	14/05	24/05	17/02	03/04	25/04	06/06	12/06	20/06
Sx 0º	0.19	0.13	0.09	-0.11	0.06	-0.01	0.51*	0.40*	0.31*	0.23*	0.22*	0.20*
Sx 45º	0.15	-0.02	0.00	-0.16	-0.08	-0.09	0.36*	0.25*	0.17	0.12	0.12	0.12
Sx 90º	0.12	-0.14	-0.07	0.11	-0.11	-0.03	-0.15	-0.15	-0.10	-0.09	-0.09	-0.10
Sx 135º	0.02	-0.05	0.05	0.26*	0.01	0.11	-0.27*	-0.19	-0.10	-0.06	-0.06	-0.06
Sx 180º	0.02	0.14	0.15	0.38*	0.17	0.21*	-0.19	-0.08	0.02	0.08	0.08	0.12
Sx 225º	0.12	0.29*	0.26*	**0.44***	**0.32***	**0.23***	0.06	0.18	0.26*	0.29*	0.29*	0.31*
Sx 270º	0.20*	**0.33***	**0.34***	0.26*	0.27*	0.21*	0.48*	**0.52***	**0.49***	**0.45***	**0.42***	**0.43***
Sx 315º	**0.22***	0.26*	0.27*	0.01	0.22*	0.12	**0.56***	0.50*	0.41*	0.34*	0.32*	0.33*

795

796 **Table 2:** Pearson's r coefficients between SD and *Sx*, calculated for the eight studied wind

797 directions over the survey days. * marks those correlations that were statistically significant

798 ($\alpha<0.05$) in at least the half of the samples (500 out of 1000 samples) from the Monte Carlo

799 approach, and bold r coefficients represent the best correlated *Sx* direction for a specific

800 survey day.

801

	Snow season 2012						Snow season 2013					
	22/02	02/04	17/04	02/05	14/05	24/05	17/02	03/04	25/04	06/06	12/06	20/06
Elev.	0.09	0.26*	0.16	0.10	0.29*	0.19	0.09	0.18	0.13	0.18	0.21*	0.26*
Slope	0.06	0.18	0.02	-0.03	0.20*	0.03	0.25*	0.27*	0.20*	0.20*	0.21*	0.26*
Curv	-0.44*	-0.45*	-0.47*	-0.49*	-0.41*	-0.37*	-0.39*	-0.40*	-0.40*	-0.39*	-0.38*	-0.38*
North	-0.06	0.00	0.04	0.19	0.07	0.11	-0.38*	-0.27*	-0.19	-0.09	-0.06	-0.11
East.	0.09	0.21*	0.13	0.13	0.13	0.11	0.25*	0.26*	0.27*	0.22*	0.18	0.14
Rad	0.05	0.04	-0.06	-0.22*	-0.12	-0.11	0.36*	0.21*	0.10	-0.09	-0.12	-0.23*
TPI 25	**-0.56***	**-0.46***	**-0.54***	**-0.58***	**-0.40***	**-0.32***	**-0.66***	**-0.68***	**-0.68***	**-0.66***	**-0.63***	**-0.61***
Sx	0.22*	0.33*	0.34*	0.44*	0.32*	0.23*	0.56*	0.52*	0.49*	0.45*	0.42*	0.43*

802

803 **Table 3:** Pearson's r coefficients between SD and the topographic variables. * marks those

804 correlations that were statistically significant ($\alpha<0.05$) in at least the half of the samples (500

805 out of 1000 samples) from the Monte Carlo approach, and bold r coefficients represent the

806 best correlated topographic variable for a specific survey day.

807

|	Snow season 2012						Snow season 2013					
	22/02	**02/04**	**17/04**	**02/05**	**14/05**	**24/05**	**17/02**	**03/04**	**25/04**	**06/06**	**12/06**	**20/06**
TPI	-0.69	-0.53	-0.60	-0.59	-0.48	-0.40	-0.78	-0.72	-0.73	-0.80	-0.74	-0.72
Sx		0.11	0.28	0.26	0.20	0.16	0.36	0.31	0.43	0.37	0.38	0.31
Elev.	0.09	0.22	0.34	0.27	0.27	0.35		0.14		0.08		0.13
Slope		-0.25	-0.29	-0.24	-0.21	-0.21		-0.10	-0.14	-0.16	-0.09	-0.15
North	-0.22	0.13	-0.16				-0.12	-0.11	-0.11			
East.	0.10						0.29	0.25	0.25	0.31	0.23	0.20
r2	0.45	0.31	0.40	0.47	0.33	0.25	0.65	0.63	0.60	0.60	0.57	0.51

808

809 **Table 4:** Multiple linear regression beta coefficients for each independent variable and

810 sampled day.

811

	Snow season 2012						Snow season 2013					
	22/02	02/04	17/04	02/05	14/05	24/05	17/02	03/04	25/04	06/06	12/06	20/06
TPI	83.2	78.8	75.0	71.7	74.0	66.9	49.1	56.4	64.4	71.2	69.9	77.5
Sx			4.6	12.7	13.4	10.8	45.9	23.1	23.0	21.8	20.1	12.5
Elev.	5.7	6.8	13.2	9.1	8.2	15.2	5.0	5.7	5.0	3.3	5.9	5.4
Slope	1.7	5.4	5.7	6.5	3.2	7.0			2.1			
North	9.3	8.1	1.5		1.3			14.7	4.3	2.4	2.9	3.6
East.									1.2	1.3	1.1	1.0
r2	0.56	0.42	0.52	0.54	0.46	0.39	0.58	0.56	0.55	0.54	0.53	0.51

812

813 **Table 5:** Contribution of the various topographic variables to the explained variance of SD

814 distribution in the binary regression tree models for 2012 and 2013. Values have been

815 rescaled from 0 to 100.

816

817

818

819

820

821

822

823

824

825

826

827

828

829

830

831

10. Figures
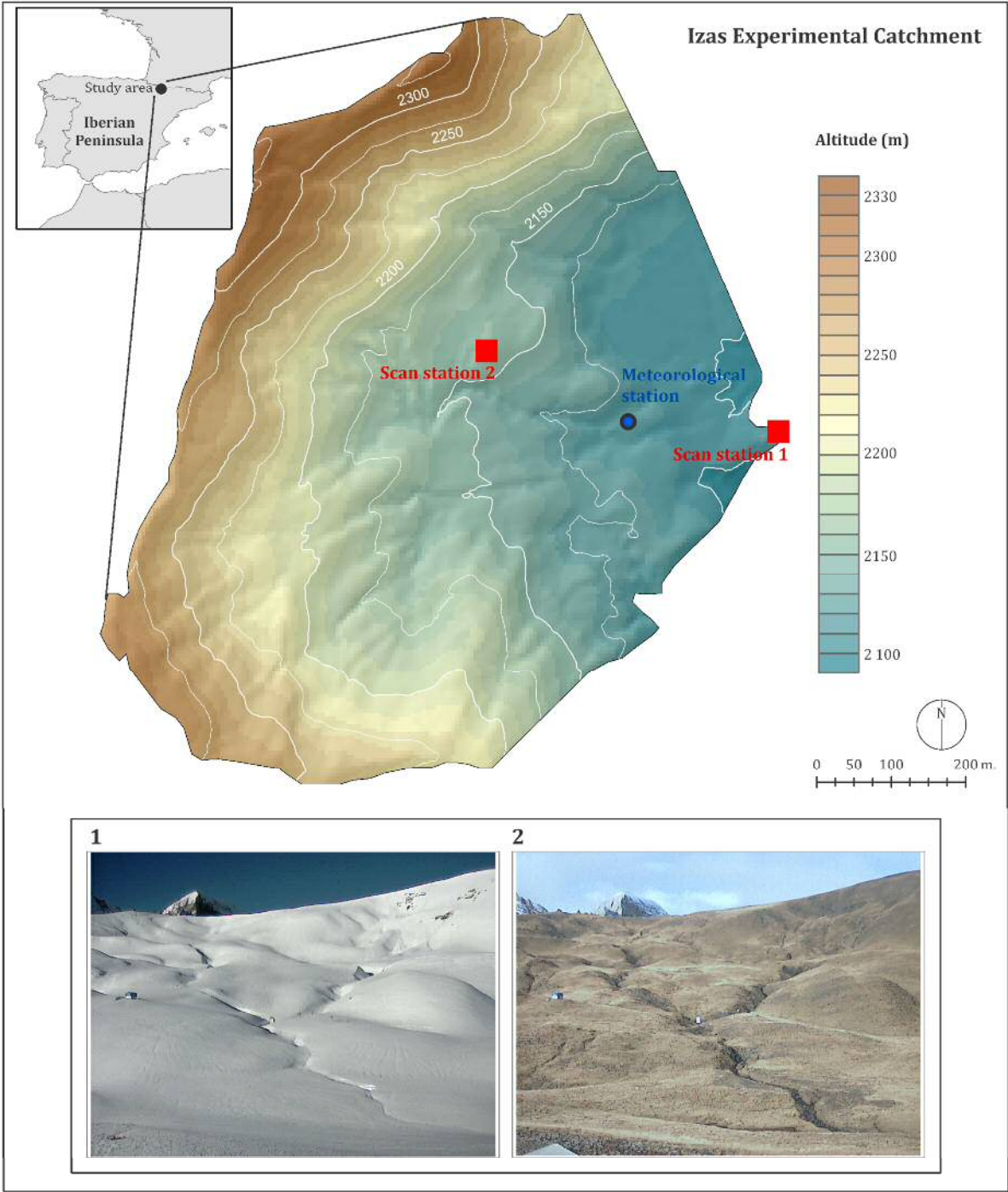
Figure 1: Location of the Izas experimental catchment, and the digital elevation model showing the positions of the scan stations and the automatic meteorological station. The two images in the bottom part of the figure, from Scan Station 1, show the terrain characteristics with (1) and without snow cover (2).
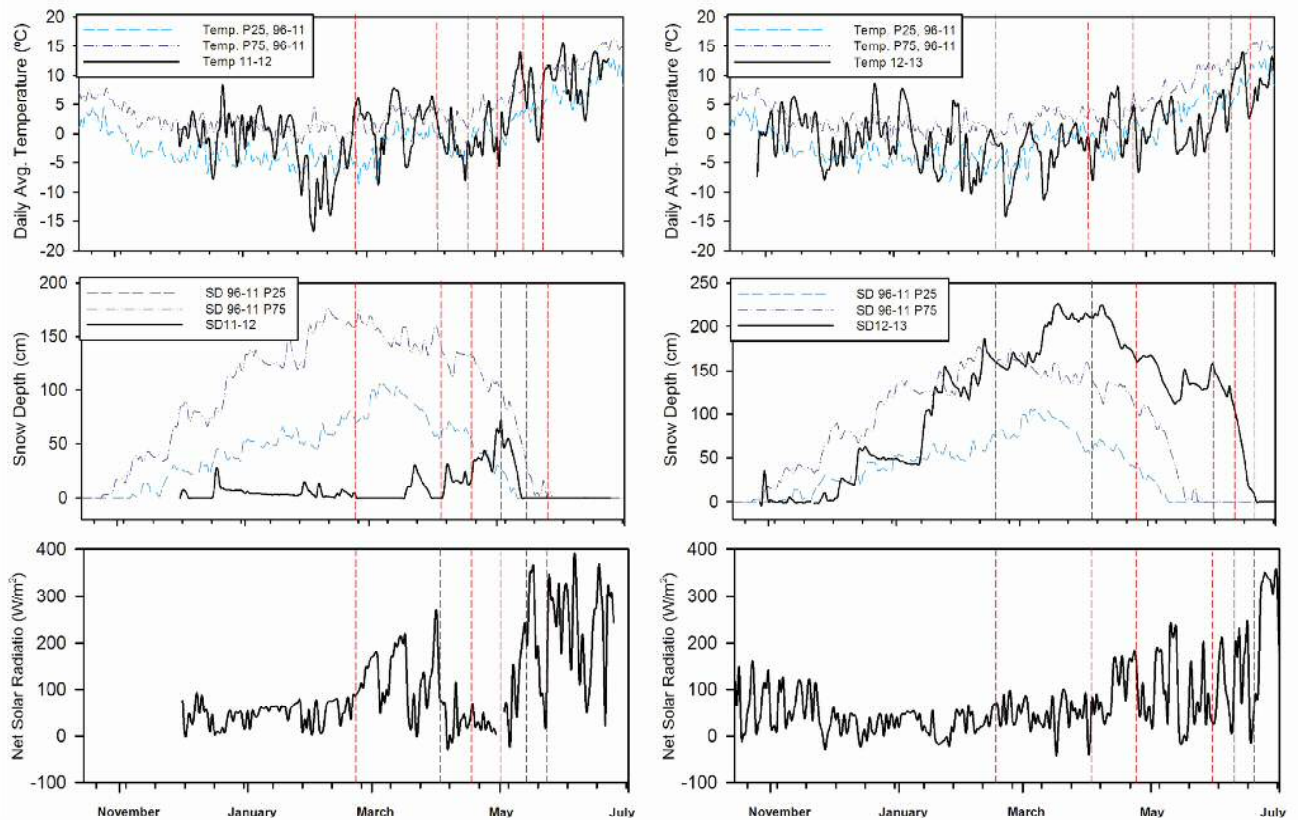
Figure 2: Daily average temperature, snow depth and net solar radiation (short wave) at the automatic weather station (AWS) for the 2012 (left) and 2013 (right) snow seasons. The continuous lines represent the daily values for 2012 and 2013, and the dashed lines show the 25th and 75th percentiles of historical daily series (1996–2011). The vertical dashed lines show the TLS survey days. Note that during some surveys no snow was present at the AWS, but some areas of the Izas experimental catchment were covered by snow.
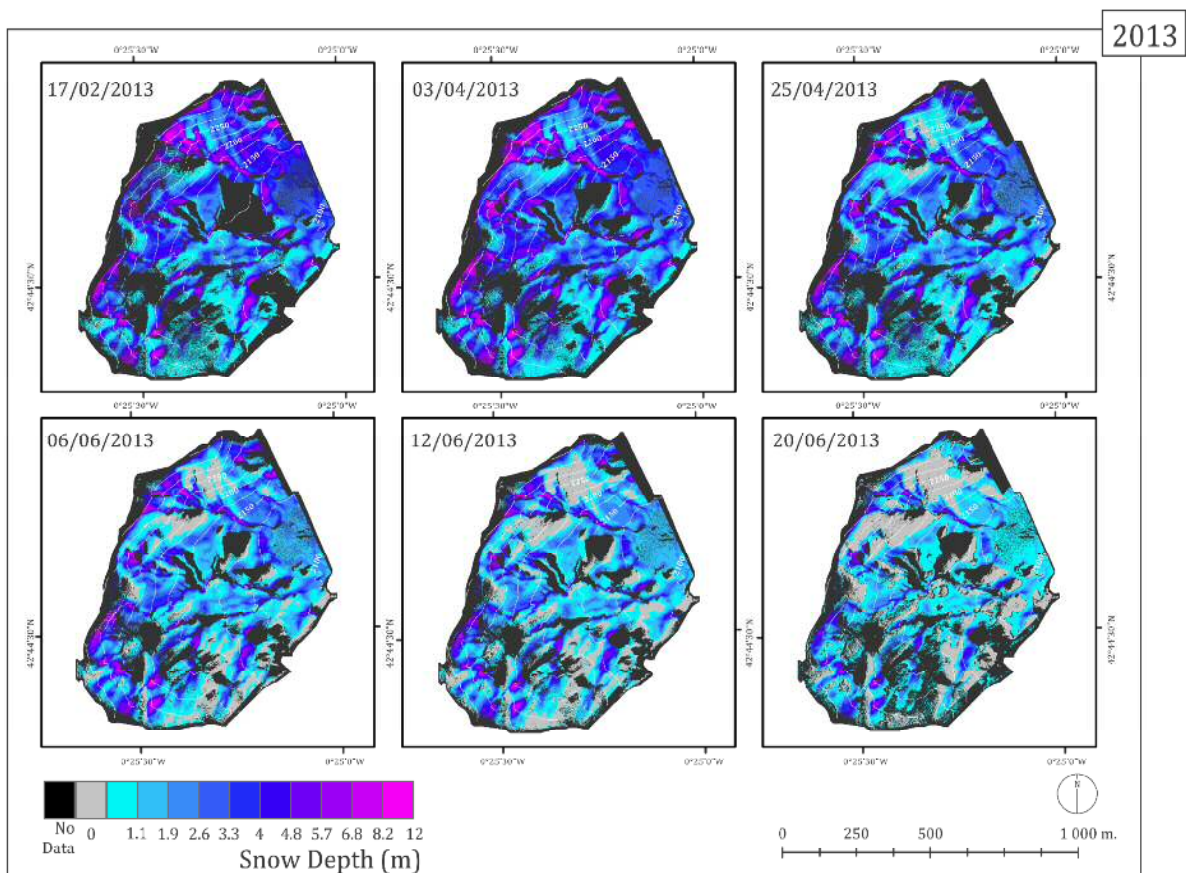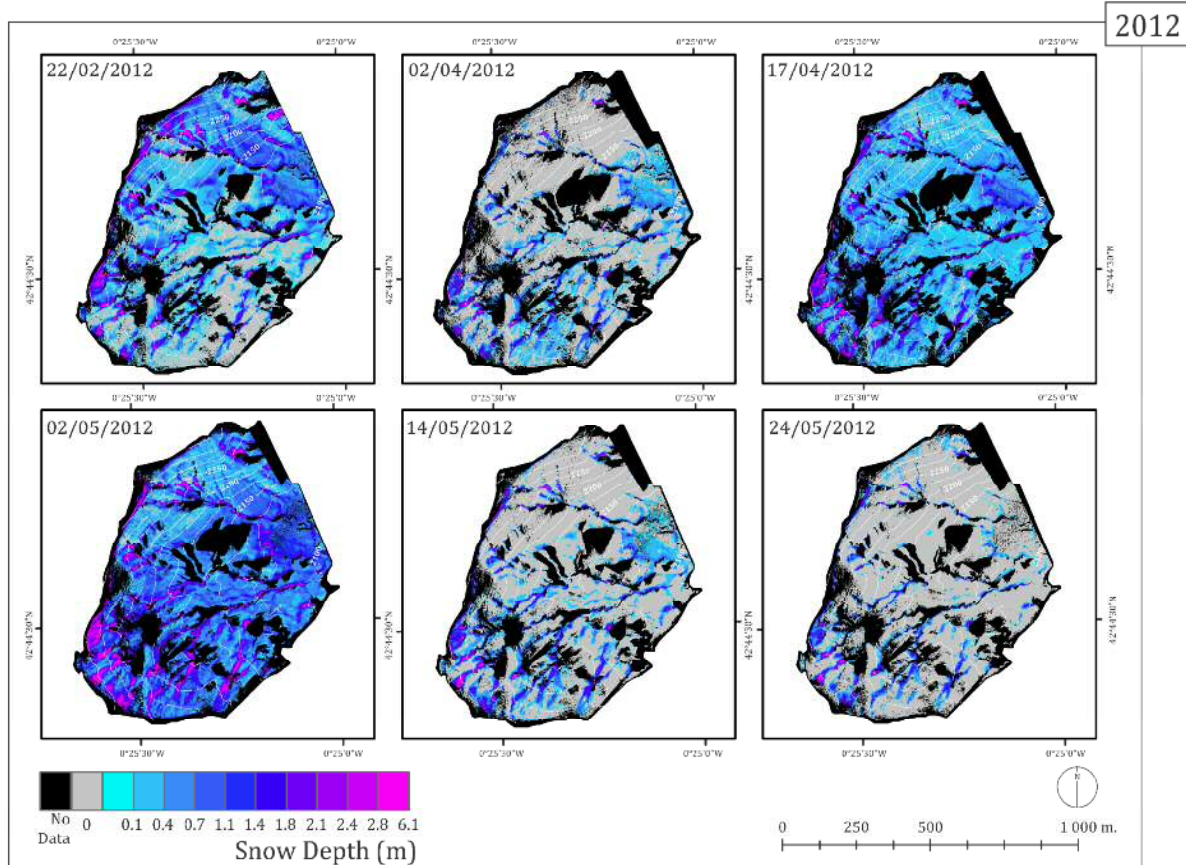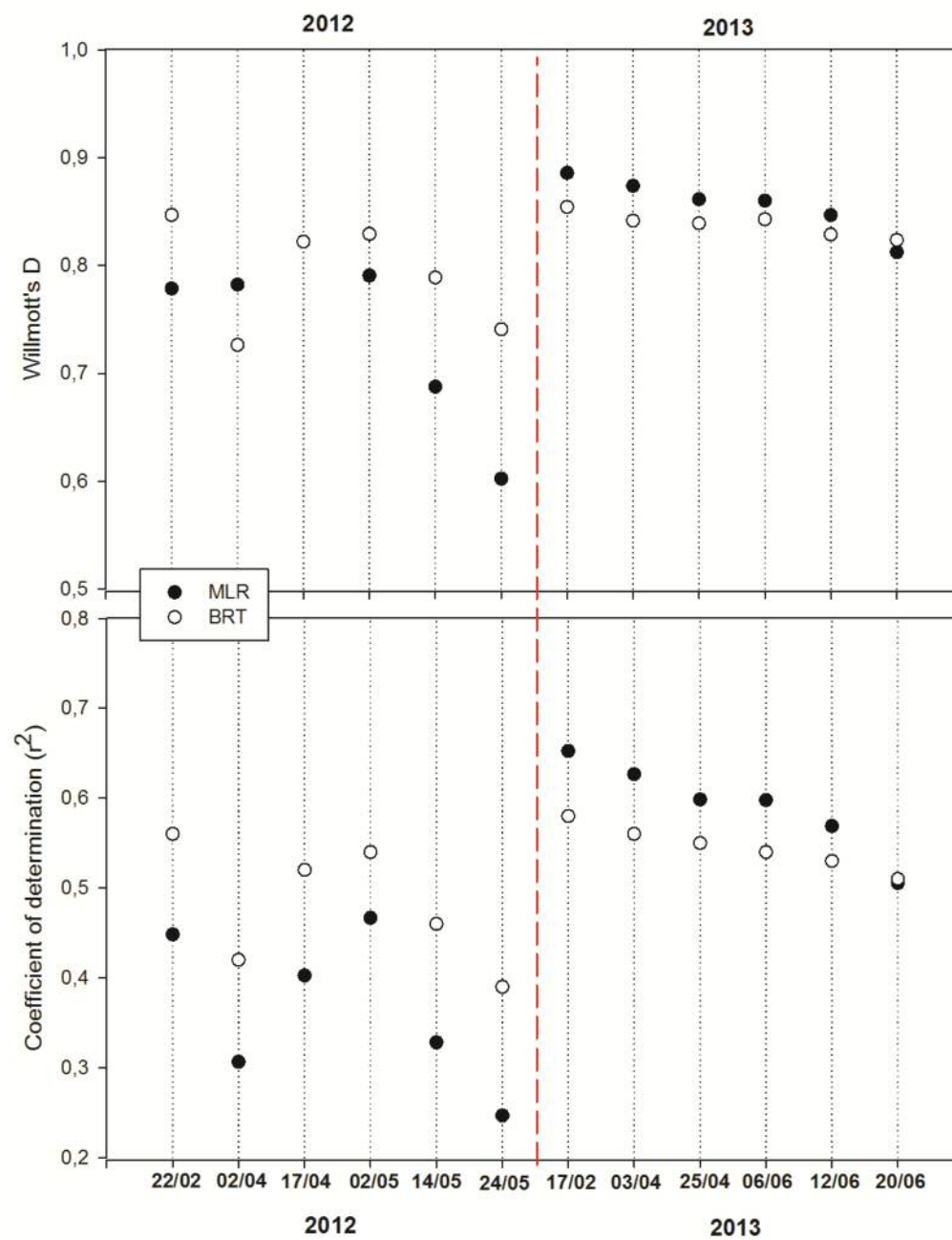
848   **Figure 3:** Spatial distribution of snow depth in the Izas experimental catchment in the surveys
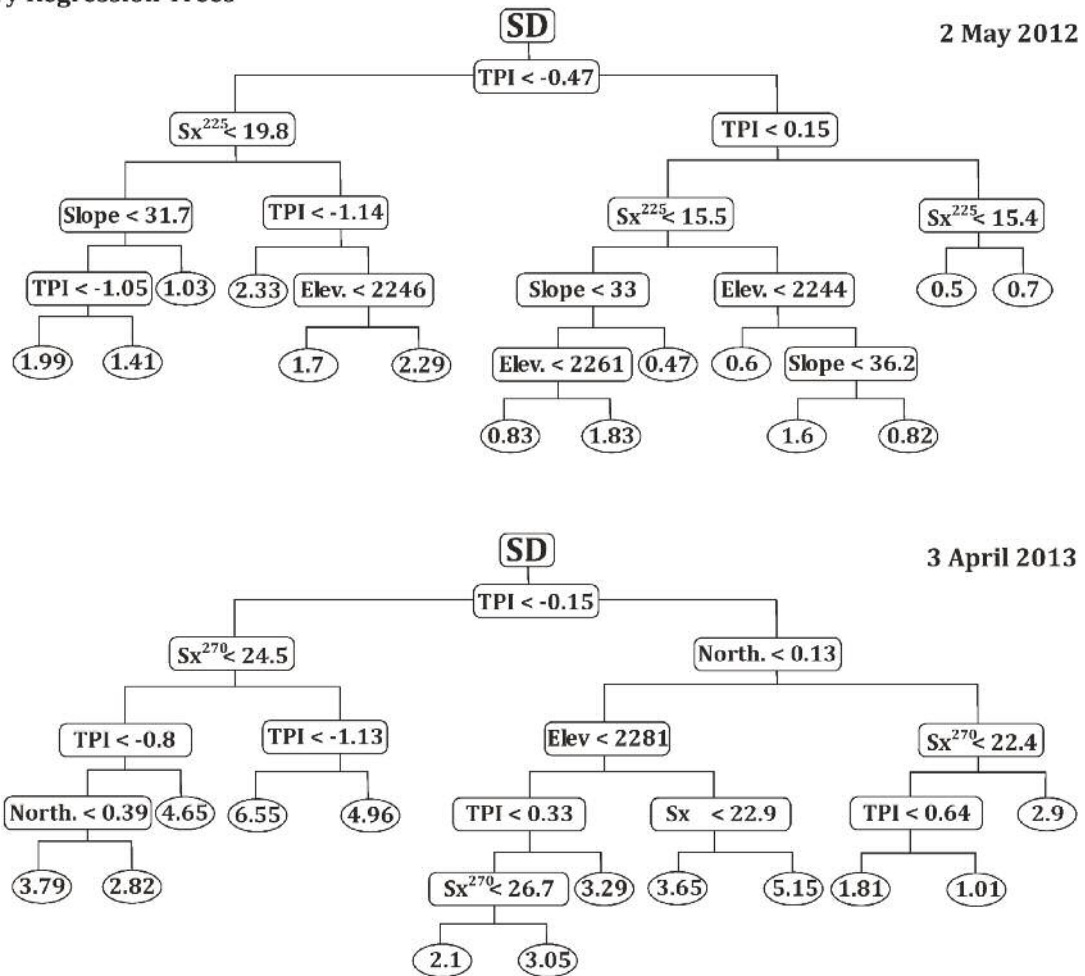
849   undertaken in 2012 and 2013.

850
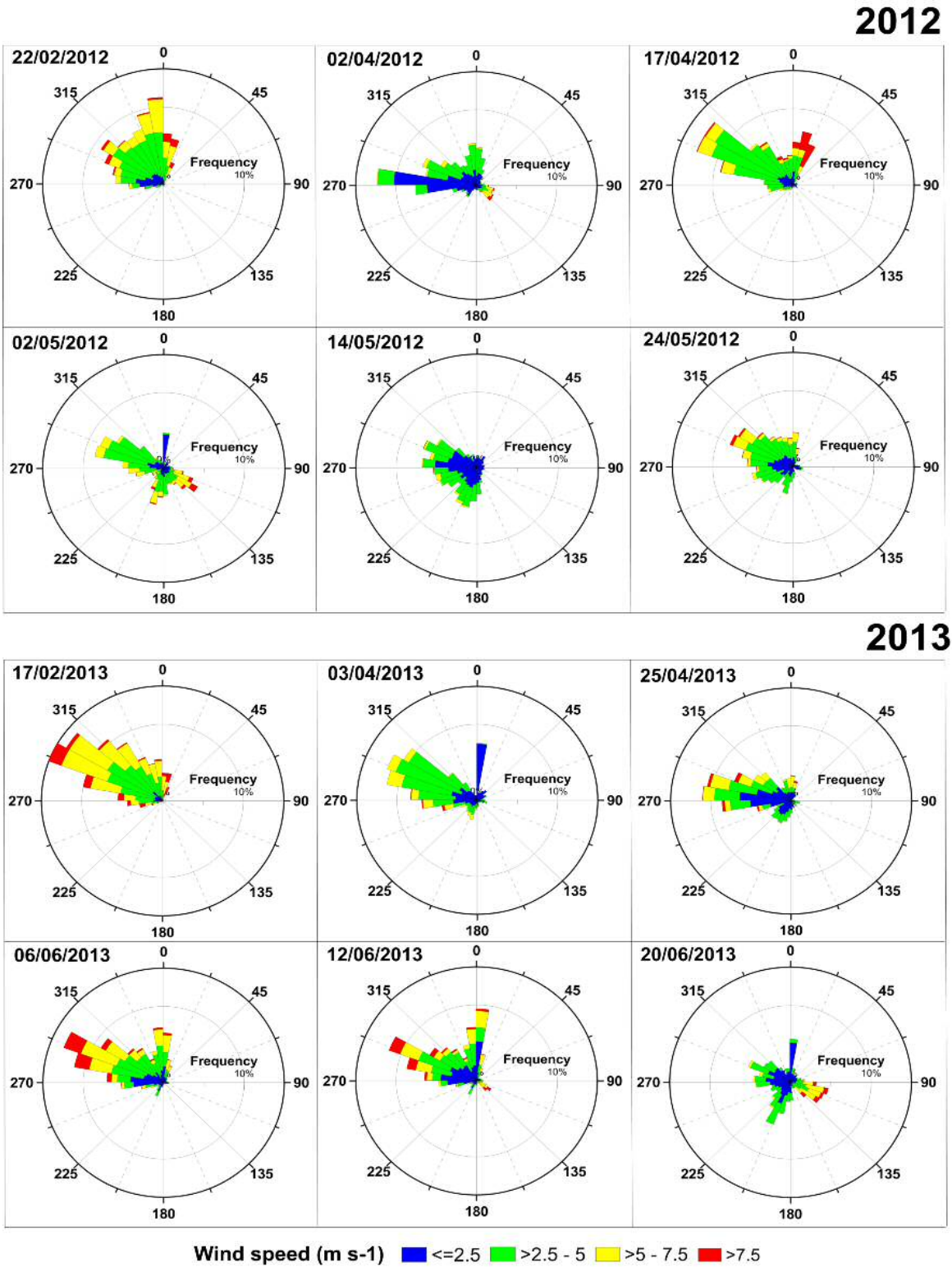
851   **Figure 4:** Wind roses from the automatic weather station placed at the catchment obtained for

852   a 15 day period.

853

854 **Figure 5:** Willmott's D and r^2 values between the observed and predicted SD, based on the

855 multiple linear and binary regression models for all survey days.

856

857

858   **Figure 6:** Binary regression tree obtained for 2 May 2012(top) and 3 April 2013 (bottom).

859   The final nodes (with ellipses) show the predicted SD in the zone having the specified terrain

860   characteristics. At each branch point, one topographic variable is considered; if the value is

861   less than the specified value, the left branch is selected, but if it is equal to or greater than the

862   specified value, the right branch is selected.

863

864

865

866
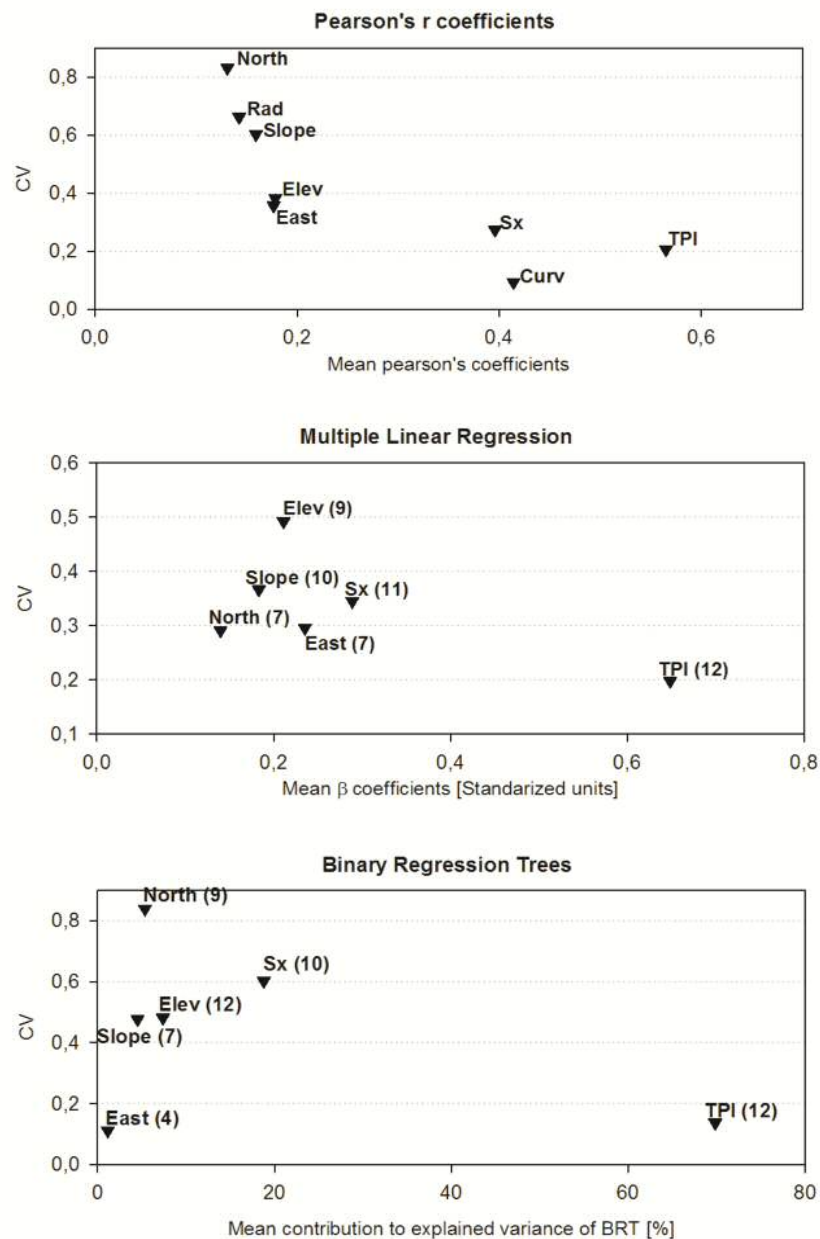
Figure 7: Mean contribution of topographic variables to models and Pearsons'r coefficients versus the coefficients of variation for all considered surveys. Upper panel shows Pearson's r coefficients; middle panel shows beta coefficients of the Multiple Linear Regression; and the bottom panel shows the contribution to the explained variance to the Binary Regression Trees. Each graph point is accompanied with its variable, and in the case of MLR and BRT, in brackets the number of days in which each variable was included in models.